



ARL-TR-8729 • JUNE 2019



Specimen Size Effects on the Compressive Stress–Strain Response of Equal Channel Angular Extrusion (ECAE) Tantalum

by Daniel Casem, Daniel Magagnosc, Jonathan Ligda,
Timothy Walter, and Brian Schuster

Approved for public release; distribution is unlimited.

NOTICES

Disclaimers

The findings in this report are not to be construed as an official Department of the Army position unless so designated by other authorized documents.

Citation of manufacturer's or trade names does not constitute an official endorsement or approval of the use thereof.

Destroy this report when it is no longer needed. Do not return it to the originator.



Specimen Size Effects on the Compressive Stress–Strain Response of Equal Channel Angular Extrusion (ECAE) Tantalum

**by Daniel Casem, Daniel Magagnosc, Jonathan Ligda, Timothy Walter,
and Brian Schuster**

Weapons and Materials Research Directorate, CCDC Army Research Laboratory

REPORT DOCUMENTATION PAGE

Form Approved
OMB No. 0704-0188

Public reporting burden for this collection of information is estimated to average 1 hour per response, including the time for reviewing instructions, searching existing data sources, gathering and maintaining the data needed, and completing and reviewing the collection information. Send comments regarding this burden estimate or any other aspect of this collection of information, including suggestions for reducing the burden, to Department of Defense, Washington Headquarters Services, Directorate for Information Operations and Reports (0704-0188), 1215 Jefferson Davis Highway, Suite 1204, Arlington, VA 22202-4302. Respondents should be aware that notwithstanding any other provision of law, no person shall be subject to any penalty for failing to comply with a collection of information if it does not display a currently valid OMB control number.

PLEASE DO NOT RETURN YOUR FORM TO THE ABOVE ADDRESS.

1. REPORT DATE (DD-MM-YYYY) June 2019		2. REPORT TYPE Technical Report		3. DATES COVERED (From - To) 1 October 2017–16 May 2019	
4. TITLE AND SUBTITLE Specimen Size Effects on the Compressive Stress–Strain Response of Equal Channel Angular Extrusion (ECAE) Tantalum				5a. CONTRACT NUMBER	
				5b. GRANT NUMBER	
				5c. PROGRAM ELEMENT NUMBER	
6. AUTHOR(S) Daniel Casem, Daniel Magagnosc, Jonathan Ligda, Timothy Walter, and Brian Schuster				5d. PROJECT NUMBER	
				5e. TASK NUMBER	
				5f. WORK UNIT NUMBER	
7. PERFORMING ORGANIZATION NAME(S) AND ADDRESS(ES) CCDC Army Research Laboratory ATTN: FCDD-RLW-PC Aberdeen Proving Ground, MD 21005-5066				8. PERFORMING ORGANIZATION REPORT NUMBER ARL-TR-8729	
9. SPONSORING/MONITORING AGENCY NAME(S) AND ADDRESS(ES)				10. SPONSOR/MONITOR'S ACRONYM(S)	
				11. SPONSOR/MONITOR'S REPORT NUMBER(S)	
12. DISTRIBUTION/AVAILABILITY STATEMENT Approved for public release; distribution is unlimited.					
13. SUPPLEMENTARY NOTES ORCIDs: Casem, 0000-0002-0475-0226; Ligda, 0000-0003-3539-8867; Magagnosc, 0000-0002-1418-9292; Schuster, 0000-0002-0791-0942; Walter, 0000-0002-1786-3668					
14. ABSTRACT Compression tests were performed on tantalum over a range of strain rates using conventional servo-hydraulic load frames and the Kolsky (split-Hopkinson pressure) bar. To obtain a large range of strain rates (0.001/s to 500k/s), different diameter Kolsky bars were required: 3.18 mm, 1.59 mm, 794 μm, and 305 μm. These different bars were used to test different sample geometries: nominally 1.6-, 0.8-, and 0.4-mm cubes, and small cylinders with 60-μm diameter and 30-μm height. It was found that the four different sample sizes led to drastically different measured strengths, even for samples tested at the same strain rates. The tantalum studied has a fine grain structure (~2 μm) so this is not believed to be due to the grain size. However, the reason for the discrepancy is unknown.					
15. SUBJECT TERMS tantalum, Kolsky bar, high-rate plasticity, split Hopkinson pressure bar, equal channel angular extrusion					
16. SECURITY CLASSIFICATION OF:			17. LIMITATION OF ABSTRACT UU	18. NUMBER OF PAGES 19	19a. NAME OF RESPONSIBLE PERSON Daniel Casem
a. REPORT Unclassified	b. ABSTRACT Unclassified	c. THIS PAGE Unclassified			19b. TELEPHONE NUMBER (Include area code) 410-306-0972

Contents

List of Figures	iv
List of Tables	iv
1. Introduction	1
2. Methods	2
2.1 Sample Fabrication	2
2.2 Miniature/Micro Kolsky Bar Techniques	3
3. Results and Discussion	4
3.1 Compressive Tests with Various Specimen Sizes	4
3.2 Isotropic Mechanical Response	6
3.3 Measurements of Impurities	7
4. Conclusion	7
5. References	9
List of Symbols, Abbreviations, and Acronyms	12
Distribution List	13

List of Figures

Fig. 1	Stress vs. strain rate for the various sample sizes tested in this program	5
Fig. 2	Compression tests at 0.001/s for specimens tested in the extrusion direction and two lateral directions. The response is largely isotropic. Specimens were 1.6-mm cubes.....	6

List of Tables

Table 1	Summary of sample geometries and the rate ranges over which they were tested	3
Table 2	Impurities measured in the three larger samples sizes.....	7

1. Introduction

In a previous paper on the rate dependence of tantalum (Ta), it was reported that the compressive response measured using two different sample sizes/shapes differed by a considerable amount, which could not be explained.¹ This report presents data on two additional sample geometries that demonstrate an even larger effect. The cause of this effect is still not understood.

The objective of the prior work was to measure the compressive stress–strain response over a wide range of strain rates (0.001/s to 500k/s). The high-rate experiments were conducted using various size Kolsky (split-Hopkinson pressure) bars. For reasons explained there and in more detail in the Methods section, it is necessary to use smaller samples and bars for progressively higher rates. Thus, the prior work used two sample sizes. The larger samples were nominally 1.6-mm cubes, tested at rates from 0.001/s to 20k/s. The smaller samples were 60- μ m-diameter, 30- μ m-high cylinders, tested at rates from 20k/s to 500k/s. At the overlapping strain rate of 20k/s, it was found that the smaller samples were approximately 12% stronger than the larger samples. In addition, the rate hardening exhibited by the smaller samples was considerably larger than that of the larger samples. This second observation is not unreasonable, because at higher strain rates dislocation drag mechanisms become more significant and increase the rate of strain-rate hardening.² In fact, an investigation into this phenomenon was the major objective of the original work. However, the discrepancy in strength between the two sets of data at the common strain rate was concerning, as it could not convincingly be explained by the sample geometry, microstructure, or specimen equilibrium in the dynamic test. This motivated the experiments described here, which consist of additional compression tests at low (0.001/s) and high (3k/s to 25k/s) strain rates using two new sample geometries, nominally 800- and 400- μ m cubes. However, instead of resolving the discrepancy, these new tests displayed an even larger size effect than noted before.

Ta is an attractive material for this study because it is technologically relevant, exhibits a large strain-rate dependence, and has good ductility. Unfortunately, depending on processing, Ta can have a highly heterogeneous microstructure.^{3–5} In addition, because the samples needed to obtain the highest strain rates are on the order of tens of microns, a material with a small grain size is required. For these reasons, we selected as the basis for our subject material a 99.98% pure nanocrystalline Ta that had been processed by a multipass Equal Channel Angular Extrusion (ECAE) procedure described in Suveen et al.^{6*} This was then annealed to produce a homogeneous material with little texture and a 2- μ m grain size. The

*The starting material corresponds to the cast-4Bc material in Table 5 of Suveen et al.⁶

annealing was done to recrystallize the heavily deformed material, leading to a more uniform microstructure and to relieve residual stresses. In addition to Suveen et al.⁶, there is other literature relevant to the ECAE processing and subsequent annealing of this material.⁷⁻⁹

The uniaxial stress compression experiments at very high strain rates (beyond ~20k/s) on Ta are unique to this work. However, a fair amount has been published on the behavior of Ta at lower rates (see, for example, Rittel et al.¹⁰ and Hoge and Mukherjee¹¹). Additional high-rate data relevant to the deviatoric (shear) behavior include pressure-shear-plate-impact experiments by Duprey and Clifton¹² and shear strength measurements under shock loading.¹³ These techniques differ from the uniaxial stress experiments in that they include a large pressure component but do provide strength information at very high rates of deformation. In none of the literature surveyed was a size effect similar to that described here noted. Any specimen variation that is reported is clearly attributable to heterogeneous microstructure, for example.¹⁴

The remaining report is structured as follows. The Methods section gives specific details of the specimen fabrication and their impurity content. It also gives details of the Kolsky bar testing and guidelines for using smaller bars and samples to obtain valid results at the higher than usual strain rates. The following section presents data for the new sample geometry and compares them to the previously published data. It also contains previously unpublished data showing that the mechanical response is largely isotropic and points out a few minor peculiarities with the micro Kolsky bar testing that can lead to small errors in the data. Suggestions for future work are included in the Conclusion.

2. Methods

2.1 Sample Fabrication

The material processing and its subsequent annealing are described in Casem et al.,¹ which also shows electron backscatter diffraction maps of the final microstructure (after heat treatment but prior to testing). All samples were machined from adjacent cross sections removed from the center of the original billet as shown in Casem et al.¹ Data from four sample geometries are considered: the original 1.6-mm cubes and 30- μm cylinders, and the two additional intermediate sizes, which are nominally 800- and 400- μm cubes. Like the larger cubes, these are made by electrical discharge machining oversized samples and polishing to final dimensions. To summarize, Table 1 gives descriptions of the samples and the rate range over which they were tested. The data are presented in the Results section.

Table 1 Summary of sample geometries and the rate ranges over which they were tested

Designation	Geometry	Typical size (mm)	Fabrication	Rate range (1/s)
1.6 mm	Cube	1.6 gage \times 1.4 \times 1.5	EDM + polishing	0.001–20k
800 μ m	Cube	0.8 gage \times 0.7 \times 0.75	EDM + polishing	0.001–30k
400 μ m	Cube	0.4 gage \times 0.35 \times 0.38	EDM + polishing	15k–40k
30 μ m	Cylinder	D = 0.060, L = 0.030	fs laser + FIB	20k–500k

2.2 Miniature/Micro Kolsky Bar Techniques

Procedures for conventional Kolsky bar testing are well known (see, for example, Chen and Song¹⁵). The main difference between miniature bars and conventional bars is the optical instrumentation, which is detailed in Refs 16–21. Four bars are used here; all are made from various grades of tool steel and have diameters of 1.59, 3.18, 0.794, and 0.305 mm. An example using the 794- μ m-diameter bar is given in the following section.

Next, we describe guidelines for deciding which bar and specimen combination to use to obtain valid data at a desired strain rate. These guidelines are based on years of experience with Kolsky bar experiments and simulations aimed at achieving valid data. There are two assumptions in the analysis of a Kolsky bar test that compel a reduction of bar diameter and sample size to obtain higher strain rates. The first is the assumption of 1-D uniaxial stress-wave propagation within the bars. For a bar wave to truly be 1-D, the wavelengths must be very large in comparison to the diameter of the bar. For any given bar, as strain rate is increased, the time needed to achieve a desired total specimen strain is reduced. Eventually, there comes a point where this assumption is violated. Thus, we require the following:

$$\lambda \geq nD. \quad (1)$$

Here λ is the wavelength of the *relevant* portions of the input, reflected, and transmitted pulses (i.e., the portion that carries useful information about the mechanical response of the sample [e.g., before failure]), and D is the diameter of the bar. Ideally, n is a large number. Assuming a reasonably constant specimen strain rate, $\dot{\epsilon}$, and a reasonable maximum strain of interest, ϵ_0 , the duration of the experiment can be estimated.

$$\Delta t = \epsilon_0 / \dot{\epsilon}. \quad (2)$$

The wavelength of the bar signals is then $= c_b \Delta t$, where c_b is the bar wave speed. Combining these three equations gives a maximum strain rate that can be obtained with a given bar diameter.

$$\dot{\epsilon} \leq \frac{c_b \epsilon_0}{nD}. \quad (3)$$

In practice, we use $n = 5$ for steel bars (Poisson's ratio ~ 0.26). Bars with lower or higher Poisson's ratio, which would be either less or more affected by dispersion, would use a different n . In most cases in this report, stress is reported at 0.07 true strain, so if this value is used in Eq. 3 with a bar wave speed of 5100 m/s, the maximum strain rates achievable using our 3.18-mm, 1.59-mm, 794- μm , and 305- μm -diameter bars are 23k/s, 46k/s, 91k/s, and 240k/s.

The next assumption that must be considered relates to specimen equilibrium. It is assumed that the sample is in a state of quasi-static equilibrium (i.e., the loading is slow enough that the wave propagation that occurs within the sample can be ignored). The simplest approach (which ignores the effects of the slower-moving plastic waves) is to require a certain minimum number of elastic wave reverberations within the sample, m . If the elastic wave speed in the sample is c_s , the time for the wave to travel the gage length L is L/c_s . Loading time is related to the strain rate by Eq. 2, so a maximum strain rate can be calculated based on considerations of sample equilibrium.

$$\dot{\epsilon} \leq \frac{c_s \epsilon_0}{mL}. \quad (4)$$

For the samples given in Table 1, with gage lengths $L = 1.6, 0.8, 0.4,$ and 0.03 mm, the limiting rates are 29k/s, 58k/s, 120k/s, and 1.6M/s. For any given specimen/bar combination, the lower rate dictates the maximum rate achievable.

3. Results and Discussion

3.1 Compressive Tests with Various Specimen Sizes

Figure 1 repeats the results of Casem et al.¹ in terms of true stress as a function of true strain rate. Stress and rate are measured at 0.07 true strain for all cases except the two highest rates (360k/s and 540k/s). Because it was felt that specimen equilibrium in these two cases was not adequate for an accurate measurement (and would violate the guidelines described previously), the reported stresses and rates for these two data points were taken at true strains of 0.11 and 15, respectively.* The light blue markers represent data from the 1.6-mm samples and the orange from

* In Casem et al.,¹ it was incorrectly reported that all of the data were measured at 0.07 true strain, without mentioning these two exceptions.

the 30- μm samples. The discrepancy of approximately 100 MPa at the overlapping rate of 20k/s is obvious. Also, the rate hardening exhibited by the smaller samples is larger than that of the larger samples, as seen by the slopes of the curve fits on the semi-log plot.

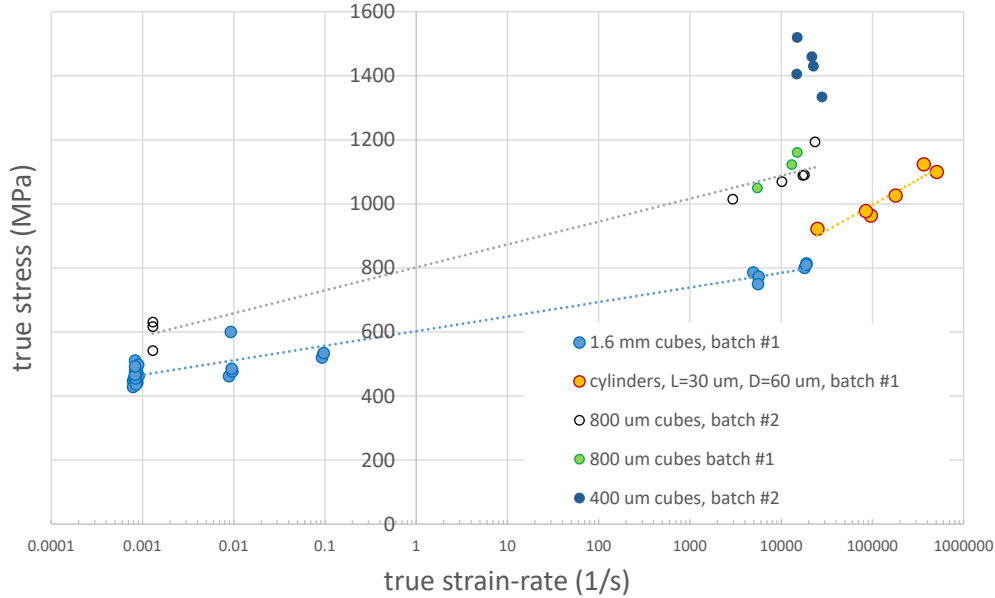


Fig. 1 Stress vs. strain rate for the various sample sizes tested in this program

Ideally, we would be able to compare other stress–strain curves from these two sample sizes at additional strain rates to see if the discrepancy persists. Unfortunately, it is not possible to conduct experiments with the larger samples at higher rates because 20k/s is about the upper limit of strain rates accessible by this sample size. Similarly, due to a lack of equipment at the time of these experiments, experiments at lower rates could not be conducted with the 30- μm samples. It was therefore decided to perform experiments with the 800- and 400- μm cubes. These could be tested at low rates and also, using both 1.6-mm and 794- μm -diameter bars, potentially, as high as 100k/s. The new data, also shown in Fig. 1, show an even stronger size effect than the prior work. Consider the open circles, representing data from the 800- μm specimens. They are stronger than the 1.6-mm specimens at both high and low rates. The hardening rate, seen in the figure as the gray dashed line, is different from either of the original data sets.

The green markers represent additional data from 800- μm samples. However, these samples were made by polishing some of the remaining 1.6-mm (untested) samples to the 800- μm dimension. This was done to make sure that there was not some difference in material between the 1.6-mm size and the 800- μm size due to an unknown error in the specimen fabrication process. However, since they fall in close agreement with the other 800- μm samples, this does not seem to be the case.

The final set of data is for the 400- μm cubes, which were tested in both the 1.6-mm and 800- μm bars. Additional increases in strength and scatter were also observed.

In all cases for the data in Fig. 1, samples were tested in the same orientation: the compression axis corresponds to the extrusion direction of the original ECAE rod. All loading surfaces were lubricated with molybdenum disulfide (MoS_2) grease (low- and high-rate experiments with samples 800 μm or larger) or vacuum grease (all experiments with samples 400 μm or smaller).*

3.2 Isotropic Mechanical Response

Most experiments performed on this material were conducted in the extrusion direction. However, a small number of experiments were performed in the lateral directions and confirm that the mechanical behavior is isotropic. Figure 2 shows these data. All samples were 1.6-mm cubes, and the tests were conducted in a servo-hydraulic load frame at strain rates of 0.01/s. The designations x and y refer to directions orthogonal to the extrusion direction in the obvious way for the original square cross-section part.†

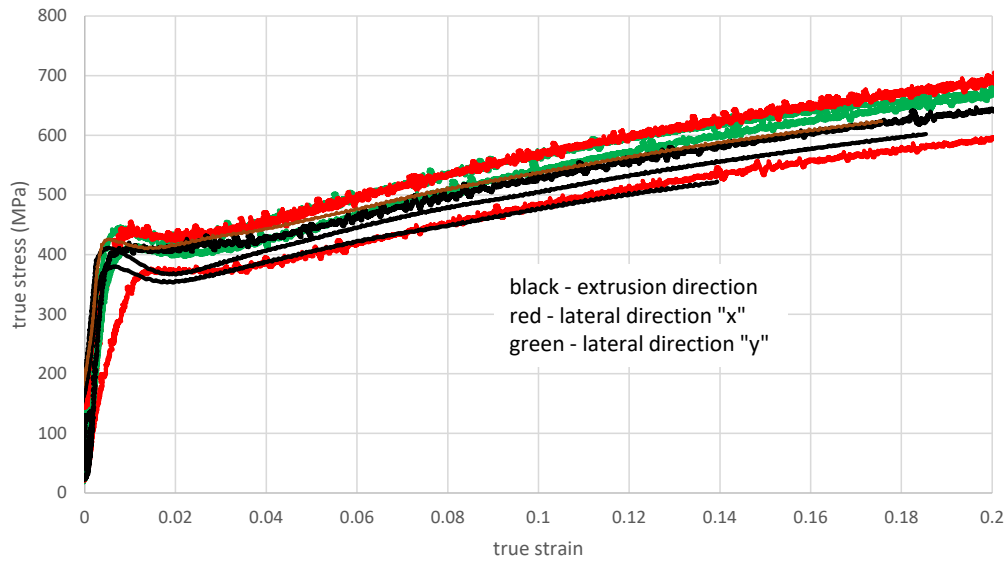


Fig. 2 Compression tests at 0.001/s for specimens tested in the extrusion direction and two lateral directions. The response is largely isotropic. Specimens were 1.6-mm cubes.

* Although MoS_2 grease is preferred for minimizing friction, its dark color and opaque appearance make it difficult to use with small samples. For this reason, the smallest samples are lubricated with a translucent vacuum grease.

† The relation between the x and y directions and the route used in the ECAE process are not known.

3.3 Measurements of Impurities

Since impurities can strongly affect the strength of Ta,²² the impurity content of the three larger sample sizes was measured. After cutting specimens to dimension and annealing under high vacuum, the oxygen (O), hydrogen (H), and nitrogen (N) content was measured by inert gas fusion using a Leco ONH836. High-purity nickel was used as a reference material. For each sample size, several specimens were combined to achieve a target total analysis mass of 0.1 to 0.14 g. Each specimen size was analyzed a minimum of three times. The resulting O, N, and H content is summarized in the Table 2. From the chemical analysis, no systematic differences in O, N, or H content are found with respect to sample size. While oxygen is known to influence the strength in Ta, the lack of apparent correlation in O content with size suggests that oxygen is not the root cause of the size effect observed here.

Table 2 Impurities measured in the three larger samples sizes

Measurements	Oxygen (ppm)	Nitrogen (ppm)	Hydrogen (ppm)
1.6 mm	375±33	25.4±5.5	9.14±0.1
800 μm	758±35	24.8±3.7	4.97±1.2
400 μm	628±43	16.1±2.7	17.6±2.0

4. Conclusion

The major finding of this report is a strong specimen size dependence of the measured stress–strain curves of the ECAE Ta studied. We have not found similar reports of this effect in the literature. The general trend is that smaller specimens are stronger, with the exception of the smallest microscale samples, which are more in line with the strength of the largest samples. We have attempted to rule out the more obvious explanations. For example, although most of the data presented here are at high rates, the effect does not seem to be an artifact of our high-rate-testing methodology. Even at the highest strain rates, we measure good sample equilibrium (refer to Casem et al.¹) and care is taken not to use the bars beyond their capabilities. Furthermore, the effect exists at low rates between the 1.6-mm and 800-μm size, although to a lesser extent than observed at higher strain rates. It does not seem to be related to impurity levels or to the specimen microstructure. The grain size of this material is 2.2 μm, so even the smallest samples contain thousands of grains. While heterogeneous behavior of Ta due to texture banding has been reported,^{3–5} this material was specifically selected to avoid this possibility. Also, it was shown in Casem et al.¹ that specimens selected randomly throughout a cross section give nominally the same stress–strain response, and it was shown here that the material

is isotropic. We have not noticed this effect with other materials tested using essentially the same procedures and specimen fabrication processes.^{23,24}

Unfortunately, the complications introduced by the unexpected results described herein are not conducive to achieving our objective of studying the rate response of Ta over a wide range of strain rates. Therefore, research on this material has been discontinued. However, the effect is interesting and could be explored by a systematic study of different sample sizes both mechanically and microstructurally. This should emphasize, at least initially, experiments at low rates to avoid the additional complications introduced by high-rate testing.

5. References

1. Casem D, Magagnosc D, Ligda J, Schuster B, Walter T. Mechanical behavior of Ta at extreme strain-rates. In: Kimberley J, Lamberson L, Mates S, editors. Dynamic behavior of materials, volume 1. Conference Proceedings of the Society for Experimental Mechanics Series. Cham (Switzerland): Springer; 2019.
2. Gilman JJ. Micromechanics of flow in solids. New York (NY): McGraw-Hill; 1969.
3. House J, Flater P, Harris R, De Angelis R, Nixon M, Bingert J, O'Brien J. Annealing and mechanical properties of ECAP tantalum. Wright-Patterson AFB (OH): Air Force Research Laboratory (US); 2011 Mar. Report No.: AFRL-RW-EG-TR-2011-045.
4. Flater PJ, House JW, O'Brien JM, Hosford WF. High strain-rate properties of tantalum processed by equal channel angular pressing. AIP Conference Proceedings. 2007;955(1):517–520.
5. Buchheit E, Cerreta L, Diebler S, Chen R, Michael J. Albuquerque (NM): Sandia National Labs; 2014. Report No.: AND2014-17645.
6. Suveen N, Mathaudhu K, Hartwig T. Grain refinement and recrystallization of heavily worked tantalum. Materials Science and Engineering: A. 2006;426(1–2):128–142. ISSN 0921-5093, <https://doi.org/10.1016/j.msea.2006.03.089>.
7. Wei Q, Jiao T, Mathaudhu SN, Ma E, Hartwig KT, Ramesh KT. Microstructure and mechanical properties of tantalum after equal channel angular extrusion (ECAE). Mater Sci Eng A. 2003;358:266–272.
8. Wei Q, Ramesh KT, Kecskes L, Mathaudhu SN, Hartwig KT. Ultrafine and nanostructured refractory metals processed by SPD: microstructure and mechanical properties. Mater Sci Forum. 2008;579:75–90.
9. Wei Q, Schuster BE, Mathaudhu SN, Hartwig KT, Kecskes LJ, Dowding RJ, Ramesh KT. Dynamic behaviors of body-centered cubic metals with ultrafine grained and nanocrystalline microstructures. Mater Sci Eng A. 2008;493(1–2):58–64.
10. Rittel D, Bhattacharyya A, Poon B, Zhao J, Ravichandran G. Thermomechanical characterization of pure polycrystalline tantalum. Materials Science and Engineering: A. 2007;447(1–2):65–70. ISSN 0921-5093, <https://doi.org/10.1016/j.msea.2006.10.064>.

11. Hoge KG, Mukherjee AK. *J Mater Sci.* 1977;12:1666–1672.
12. Duprey KE, Clifton RJ. *AIP Conference Proceedings*; 1988;429:475–478.
13. Gray GT III, Bourne NK, Millett JCF. Shock response of tantalum: lateral stress and shear strength through the front. *Journal of Applied Physics.* 2003;94:6430. doi: 10.1063/1.1620679.
14. Wei Q, Pan ZL, Wu XL, Schuster BE, Kecskes LJ, Valiev RZ. Microstructure and mechanical properties at different length scales and strain rates of nanocrystalline tantalum produced by high-pressure torsion. *Acta Materialia.* 2011;59(6):2423–2436.
15. Chen W, Song B. *Split Hopkinson (Kolsky) Bar.* New York (NY): Springer; 2011.
16. Casem DT. A small diameter Kolsky bar for high-rate compression. *Proc. of the 2009 SEM Annual Conference and Exposition on Experimental and Applied Mechanics*; 2009 June 1–4; Albuquerque, NM.
17. Casem DT, Grunschel SE, Schuster BE. Normal and transverse displacement interferometers applied to small diameter Kolsky bars. *Exp Mech.* 2012;52(2):173–184.
18. Huskins EL, Casem DT. Compensation of bending waves in an optically instrumented miniature Kolsky bar. *Journal of Dynamic Behavior of Materials.* 2012.
19. Casem, DT, Zellner M. Kolsky bar wave separation using a photon Doppler velocimeter. *Experimental Mechanics.* 2013;53:1467–1473.
20. Casem DT, Huskins EL, Ligda J, Schuster BE. A Kolsky bar for high-rate micro-compression – preliminary results. *Proc. 2015 SEM Annual Conference and Exposition*; 2015 June; Costa Mesa, CA.
21. Casem DT, Ligda JP, Schuster BE, Mims S. High-rate mechanical response of aluminum using miniature Kolsky bar techniques. In: Kimberley J, Lamberson L, Mates S, editors. *Dynamic behavior of materials, vol. 1. Conference Proceedings of the Society for Experimental Mechanics Series.* Springer; 2018.
22. Smialek RL, Mitchell TE. Interstitial solution hardening in tantalum single crystals. *The Philosophical Magazine: A Journal of Theoretical Experimental and Applied Physics.* 1970;22(180):1105–1127. doi: 10.1080/14786437008226921.

23. Casem DT, Weerasooriya T, Walter TR. J Dynamic Behavior Mater. 2018;4(1):138–149. <https://doi.org/10.1007/s40870-018-0142-x>.
24. Casem D, Ligda J, Walter T, Darling K, Hornbuckle B. Strain-rate sensitivity of Cu-10Ta to 700k/s. Journal of Dynamic Behavior of Materials. In review, 2019.

List of Symbols, Abbreviations, and Acronyms

1-D	one-dimensional
ECAE	Equal Channel Angular Extrusion
H	hydrogen
MoS ₂	molybdenum disulfide
N	nitrogen
O	oxygen
Ta	tantalum

1 DEFENSE TECHNICAL
(PDF) INFORMATION CTR
DTIC OCA

2 CCDC ARL
(PDF) IMAL HRA
RECORDS MGMT
FCDD RLD CL
TECH LIB

1 GOVT PRINTG OFC
(PDF) A MALHOTRA

1 CCDC ARL
(PDF) FCDD RLW PC
D CASEM